RSC Advances

ROYAL SOCIETY OF CHEMISTRY

www.rsc.org/advances

Graphical Abstract

A DFT study on structure, stabilities and electronic properties of double Magnesium doped Gold clusters

Debajyoti Bhattacharjee, Bhupesh Kr. Mishra and Ramesh Ch. Deka*

Department of Chemical Sciences, Tezpur University, Napaam, Assam 784 028, India

*Corresponding author, Fax: +91 3712267005. Email address: ramesh@tezu.ernet.in (R.C.D.)

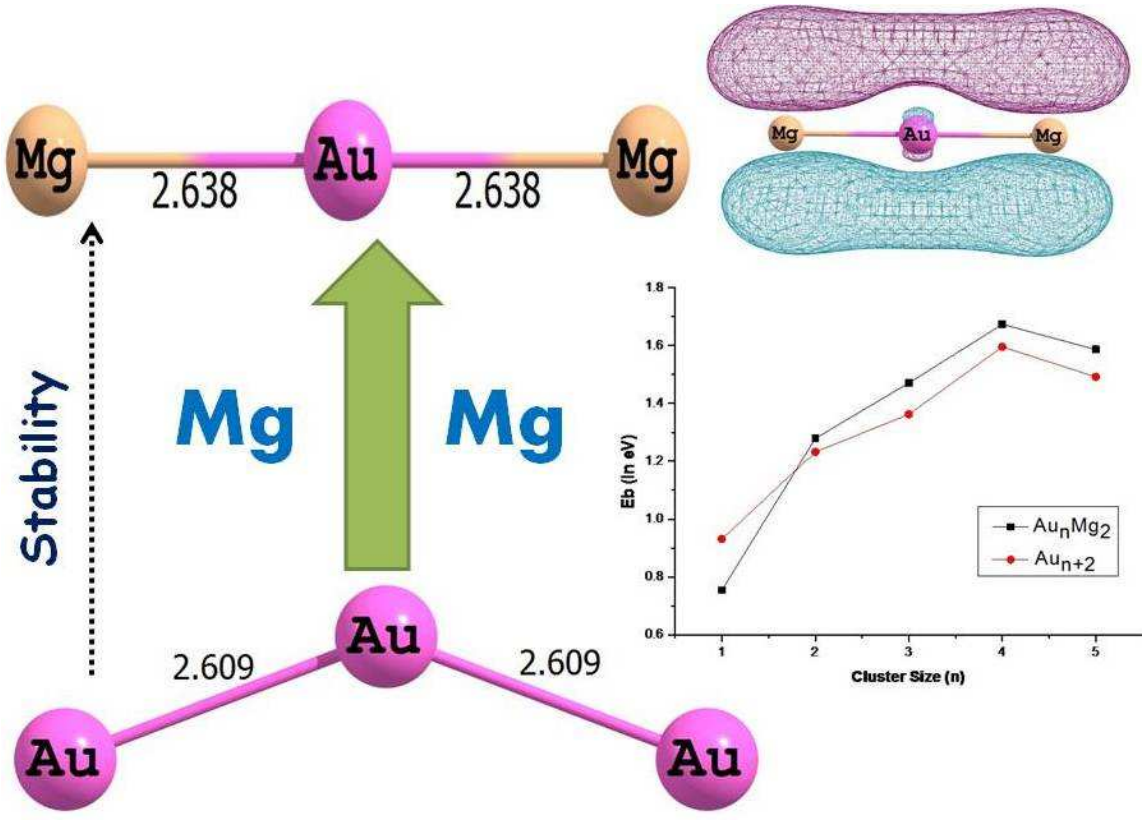

The doping of two Mg atoms on Au-clusters has considerable effects on the structure and stability of gold clusters. The stability on the doped clusters enhances the stability of pure Au-clusters as observed from the binding energy plot.

A DFT study on structure, stabilities and electronic properties of double Magnesium doped Gold clusters

Debajyoti Bhattacharjee, Bhupesh Kr. Mishra and Ramesh Ch. Deka*

Department of Chemical Sciences, Tezpur University, Napaam, Assam 784 028, India

*Corresponding author, Fax: +91 3712267005. Email address: ramesh@tezu.ernet.in (R.C.D.)

Abstract

Density functional theory (DFT) with PW91PW91 functional have been applied to investigate the structures, relative stabilities and electronic properties of small bimetallic neutral, cationic and anionic Au_nMg_2 (n=1-5) clusters. The results show that doping with two Mg atoms dramatically affects the geometries of the ground-states of Au_n (n=1-7) clusters. The relative stabilities of the clusters are compared on the basis of average binding energies, fragmentation energies and second order difference of energies. These parameters show even-odd alternation phenomenon. The electronic properties are calculated by using hardness values and this suggests that even numbered clusters are more stable than that of odd counterparts in both bare as well as doped ones. The nature of bonding interaction is also investigated by using Bader's quantum theory of atoms in molecules (QTAIM) which indicates the presence of covalent bonding in the studied clusters. The population analysis reveals the transfer of electrons from Mg to Au atoms which in turn responsible for the enhance stability of doped clusters.

Keywords: Au-Mg clusters, Density Functional Theory, Binding energy, Chemical hardness, QTAIM, Bond critical point

1. Introduction

The discovery of unusual catalytic abilities of gold nanoclusters by the revolutionary work of Haruta considerably increases the attention in the study of gold at nano level.[1] Based on this work, a large number of theoretical and experimental studies were carried out on the structural as well as catalytic property of gold nanoclusters.[2-9] It has been reported that, from Au_2 to Au_{12}, all the most possible lowest energy structures adopt planar configuration.[10] On the other hand in case of anionic clusters also, Au_4^- to Au_{12}^- exhibit planar structures[2] whereas in case of cationic, a transition from 2D to 3D occurs from Au_8^+.[5] Apart from these monometallic nanoclusters of Au, bimetallic nanoclusters also find wide interest in recent studies.[10-13] They are composed of two different metal elements and are more promising than the monometallic nanoparticles because synergestic effect is expected.[10] They show novel catalytic behaviour based on the effect of second metal element added. This effect can often be explained in terms of an ensemble[11] or a ligand effect in catalysis.[12] Recently, considerable attentions have been paid on Au clusters doped with different atoms by researchers. Wang *et al.*[13] carried out Density Functional Study on Cu doped Au clusters and compared them with pure Au clusters. They found that for neutral and anionic clusters, the structures are planar for both bare and Cu doped Au clusters. But in case of cationic clusters, a transition from 2D to 3D occurs at Au_6Cu^+. Using DFT, Manzoor *et al.*[14] studied the effect of Si doping in Au_7 and Au_8 clusters. They found that silicon doped Au_7Si cluster shows considerable binding and activation of O_2 molecule in comparison to the pristine Au_8 cluster and this fact was further confirmed by geometrical parameters (O-O and Au-O bond length) and O-O stretching frequency. Shao *et al.*[15] also carried out DFT study in Be doped cationic Au_n(n=1-8) clusters. They revealed that doping of Be can remarkably increase the stability of Au clusters as compared to bare clusters. Simillarly, Ju-Wang *et al.*[16] studied theoretically the Al doped anionic Au clusters and reported that doping with a single Al atom can dramatically affect the

ground-state geometries of the Au clusters and the stability order follows even odd alternation. Very recently, we also performed DFT and QTAIM study on Be doped Au clusters and found that Be doping can also increases the stability of Au clusters.[17]

It is well known fact that Magnesium (Mg), an alkaline earth element, is extremely reactive in the free state. It is resistance to corrosion when alloyed to certain metals like Fe, Ni, Cu, Co etc.[18] For Mg doped Au clusters, Kyasu *et al.*[19] performed anion photoelectronic study on Au_nMg^- (n=2-7) clusters. Majumdar *et al*.[20] theoretically observed the structure and bonding of Au_5Mg cluster. They found that Au_5Mg cluster adopt planar structure simillar to Au_6. In an another study, Li *et al.*[21] systematically analysed the properties of anionic Au_nMg(n=1-8) clusters and found that lowest energy structures for Au_nMg clusters are different to that of the bare Au clusters. However, to the best of our knowledge, no systematic theoretical investigations into Mg_2Au_n clusters have been performed. For example, if two Mg atoms are doped in gold clusters together, do their structures and properties differ from those of bare gold clusters? Therefore, by applying DFT we studied the structural and electronic properties of Au clusters doped with two Mg atoms, Au_nMg_2 (n=1-5). During this study, we optimised a certain type of structures by doping Mg atoms at different positions in the bare Au clusters. The importance of this work lies in the fact that nanosized Au clusters already shows tremendous catalytic activity for different types of reactions and doping of a metal can further enhanced its catalytic property. The novelity of the work with reference to the previous works lies in the facts that for the first time we have studied the all neutral and charged clusters for two Mg metal doped Au clusters and compared with the pure ones. Therefore, our present study can provide powerful guidedlines to consider the Mg doped Au clusters in the further experimental research.

2. Computational methods

The initial structure at neutral state was generated by performaing a classical simulated annealing technique using the Forcite Plus code as encoded in the MATERIAL STUDIO software.[22] The Universal force field (UFF)[23] was adopted to perform this simulation. Previous studies[24,25] have shown that UFF provides reliable results for gold based systems. The cut-off radius was chosen to be 15.5 Å and NVE ensemble was used. A total of 100 annealing structures were generated at high temperature (1000 K) and 50 heating ramps per cycle. The most stable structure obtained by this simulation was used as the input for DFT calculations.

Geometry optimizations and frequency analysis of Au_nMg_2 clusters have been performed using the GAUSSIAN 09 suits of program.[26] In the frame work of DFT, we employ the gradient-corrected exchange and correlation functional of Perdew-Wang (PW91PW91)[27] to explore the stationary points on the potential energy surface. As we all know, the relativistic effects play a primary role in the structure and energetic of Au-containing clusters, we used the Los Alamos LANL2DZ[28,29] Effective Core Pseudopotentials (ECP) and valence double-ζ basis sets for Au. The Mg atoms are treated with 6–311+G(d) basis set. PW91PW91 functional is used successfully in the study of previous Mg doped Au clusters[20,21] as well as studies on other metal clusters also.[15,30,31] We first perform calculations on Au_{n+2} (n = 2–5) clusters in order to discuss the effects of doped impurity atoms on gold clusters. Full geometry optimizations have been done for the neutral clusters as well as ionic clusters without imposing any symmetry constraints. In order to obtain the lowest energy doped isomers, initial structures were constructed substituting Au atoms by Mg atoms in the pure gold structures at various attaching sites. The most stable clusters are obtained by comparying their relative energies. The vibrational frequencies are found to be positive for all the structures confirming them to be at energy minima. The zero-point vibrational energy

corrections have been included in all the calculations. The total energies of the most stable clusters are used to determine their binding energy, relative stability, ionization potential, electron detachment energy as well as chemical hardness as a function of clusters size to describe the stability of the clusters. We analysed the nature of bonding in the studied clusters, based on Bader's quantum theory of atoms in molecules (QTAIM).[32-34] For QTAIM analysis, we have generated the wave function using Gaussian 09 at the same level of theory as employed in structure optimization and then used the AIMALL package[35] to study different bond parameters.

3. Results and Discussion

3.1 Structural study of Au_nMg_2 clusters

The various lowest energy structures for neutral and charged Au_n and Au_nMg_2 clusters are presented in Figs. 1-3. Among different isomers obtained for a particular cluster, the energy of the most stable isomer is taken as zero and energy of the others are compared relative to it.

3.1.1 Neutral clusters

The structures obtained in present work for neutral Au clusters are identcal to the previous study.[2] Moving on to doped clusters, from Fig. 1, it can be seen that the most stable structure for $AuMg_2$ is 1(1a) having a linear shape. The Au-Mg bond lengths are found to be 2.638 Å. The other isomer, 1(1b) is found to be higher in enrgy compared to 1(1a) by 0.22eV. For Au_2Mg_2 clusters, the structure 1(2a) with square planar shape is found to be most stable having symmetry, D_{2h}. Here the Au-Mg bonds are founds to be 2.614 Å. In case of Au_3Mg_2 clusters, the most stable structure is 1(3a) with symmetry C1. However, here we obtained a 3D isomer, 1(3b), which is higher in energy than 1(3a) by 0.01 eV. Thus a transition from 2D to 3D is obtained at Au_3Mg_2 for the neutral clusters. Moving on to Au_4Mg_2, the most stable

isomer is 1(4a). It has symmetry C_{2V} having shortest Au-Mg distance of 2.476 Å. This bond length is found to be in good agreement with that of 2.56 Å for the single Mg doped cluster.[20] At last a planar isomer 1(5a) having symmetry C_{2V} is found for the most stable structure of Au_5Mg_2. The calculated values of shortest Au-Mg and Au-Au bond lengths are 2.587 and 2.729 Å, respectively. However, we obeserved 2D structures for the neutral clusters except 1(3b) for which 3D is observed.

From the above discussion, it can be noted that almost all the the lowest energy structures of Mg_2Au_n favor a 2D plannar structure. It is seen from the Fig. 1 that most stable structures of Au_2Mg_2 and Au_4Mg_2 are similar to that of their bare counterpart. In addition to these stable structrues, there exist atleast one isomer which is structurally simillar to the bare Au clusters in other clusters. However, a transition from 2D to 3D is obtained at n=3 in case of doped clusters. Also, the stable isomers for Au_3Mg_2 and Au_4Mg_2 have different geometry to that of the pure gold clusters. These indicates that the doubly doped Mg atoms can affect the geometries of the ground-state of neutral Au_n clusters.

3.1.2 Charged Clusters

The different charged (cationic and anionic) isomers for Au_{n+2} and Au_nMg_2 (n = 1–5) are shown in Figs. 2 and 3. For the $AuMg_2^+$, the most stable cluster is 2(1a) having the linear shape. Similarly the stable isomers are 2(2a), 2(3a), 2(4a) and 2(5a) for $Au_2Mg_2^+$, $Au_3Mg_2^+$, $Au_4Mg_2^+$ and $Au_5Mg_2^+$, respectively as depicted in Fig. 2. Here we obtained only 2D planar structures and no any transition to 3D structure seems to occur. On comparing the doped structures with that of the bare ones, it seems that apart from $AuMg_2$ and Au_3Mg_2, the stable isomers for other clusters are found to be simillar to the bare clusters. However, various high energy isomers viz. 2(2b), 2(4c) and 2(5b) along with stable isomers of $AuMg_2$ and Au_3Mg_2 adopt different geometries to that of the pure gold counterpart. For anionic clusters, the most stable isomers are found to be 3(1a), 3(2a), 3(3a), 3(4a) and 3(5a) for $AuMg_2^-$, $Au_2Mg_2^-$,

$Au_3Mg_2^-$, $Au_4Mg_2^-$ and $Au_5Mg_2^-$, respectively (Fig. 3). It is interesting to compare the structures for anionic clusters reported in this study with that of the previous observation for single Mg doped Au-clusters.[21] It is found that all the stable isomers for doubly doped clusters are different to that of the singly doped clusters. However, the shortest Au-Mg bond lengths are found to be comparable in both the types of clusters. In this study, a transition from 2D to 3D cluster occurs at $Au_3Mg_2^-$. Also the isomers 3(3b), 3(3c), 3(4a), 3(4b), 3(4c) and 3(5c) have different geometries to those of pure gold clusters. All these results indicates that in case of charged clusters also, doubly doped Mg atoms can play a key role to effect the geometries of the ground-state Au_n clusters and also they are structurally different to that of the singly doped clusters.

3.2 Stability of Au_nMg_2 clusters

The relative stabilities of the Au_nMg_2 clusters are calculated in terms of averaged binding energies per atom, (E_b) fragmentation energies, D, and second-order difference of energies, Δ^2E, using formulae (1-7) given below. These three parameters already proved to be a powerful tool to reflect the relative stability of the clusters.

For Au_n clusters averaged binding energies $E_b(Au_{n+2})$, fragmentation energies ΔE (Au_{n+2}), and second-order difference of energies $\Delta^2E(n)$ are calculated using the following formulae:

$$E_b(Au_{n+2}) = [(n+2)E(Au) - E(Au_{n+2})]/(n+2) \quad (1)$$

$$E_b(Au_{n+2})^q = [E(Au)^q + nE(Au) - E(Au_{n+2})^q]/(n+2) \quad (2)$$

$$\Delta E\ (Au_{n+2})^q = [E(Au_{n+1})^q + E(Au) - E(Au_{n+2})^q] \quad (3)$$

$$\Delta^2 E(Au_{n+2})^q = [E(Au_{n+1})^q + E(Au_{n+3})^q - 2E(Au_{n+2})^q] \quad (4)$$

where, E(Au) represents the ground state energy of the Au, q is the charge on the cluster, q=0,+1 and -1 for neutral, cationic and anionic clusters, respectively and n is the number of gold atoms associated with the clusters.

Similarly for Au_nMg_2 clusters averaged binding energies $E_b(n)$, fragmentation energies $\Delta E(n)$ and second-order difference of energies $\Delta^2 E(n)$ are calculated using the following formulae:

$$E_b(Au_nMg_2)^q = [2E(Mg)^q + nE(Au) - E(Au_nMg_2)^q]/(n+2) \quad (5)$$

$$\Delta E(Au_nMg_2) = [E(Au_{n-1}Mg_2) + E(Au) - E(Au_nMg_2)^q] \quad (6)$$

$$\Delta^2 E\,(Au_nMg_2)^q = [E(Au_{n-1}Mg_2) + E(Au_{n+1}Mg_2) - 2E(Au_nMg_2)^q] \quad (7)$$

where, $E(Mg_2Au_n)$, E(Au), E(Mg) denote the total energy of the Mg_2Au_n, Au and Mg, respectively.

3.2.1 Binding energies per atom

The variation of calculated binding energies per atom (E_b) for the most stable isomers as a function of cluster size is shown in Fig. 4. Here we compared the binding energies of the doped clusters relative to pure gold clusters. It is observed from the figure that the binding energy per atom for the pure cluster increases with cluster size for the neutral clusters, therefore, the clusters continue to gain energy during the growth process. However, for the charged clusters, the B.E. values show an even-odd alternation. For neutral and anionic doped clusters, we obtained a sharp peak at n=4 and n=3, 5 respectively, indicating the higher stability of these clusters in the region n=1-5. However, for the cationic doped clusters, the E_b values decrease with cluster size. Comparison of binding energies reveals that doped clusters are more stable to that of pure clusters. The binding energy plots (Fig. 4) suggested that in all the neutral, cationic and anionic clusters, the doping of two Mg atoms increase the stability of the Au clusters. For the anionic clusters, we found that the variation of the binding energy plot is similar to that of the previous study on singly doped clusters.[21] It is also clear from the plot that the binding energy values are higher for doubly doped clusters to that of single ones. This indicates the enhance stability of our studied clusters. When we compare the binding

energies of charged and neutral clusters (Fig. S1 of supplementary information), the binding energy order is found to be increases as: neutral < anionic < cationic for Mg doped clusters.

3.2.2 Fragmentation energies

The variation of values of fragmentation energies for the most stable isomers as a function of cluster size is shown in Fig. 5. The fragmentation energies are sensitive to the relative stabilities that can be observed in mass abundance spectra. From Fig. 5, it can be seen that both the bare as well as doped clusters exhibit even-odd alternation with respect to cluster size. For neutral bare clusters, the clusters with even number of atoms are more stable than that with odd number of atoms. However, the reverse is observed for the charged clusters and the clusters bearing odd number of atoms are more stable. For neutral and anionic, Au_nMg_2 clusters follow same trend as observed for bare clusters and also the plot for anionic cluster is similar to the previous study.[21] For neutral clusters, a sharp peak occurs at n=4 whereas for cationic and anionic clusters, sharp peaks occur at n=2 and n=3 respectively indicating the stability of these clusters in the region n=1-5.

3.2.3 Second-order difference of energies

The second-order difference of energies (Δ^2E), generally known to provide the relative stability of a cluster of size n with respect to its neighbor. Fig. 6 provides the variation of values of fragmentation energies for the most stable isomers as a function of cluster size. Fig. 6 clearly indicates the even-odd alternation for bare as well as doped clusters. For neutral doped clusters, the cluster with n=4 shows a sharp peak indicating its higher stability. Similarly, n=2 and n=4 shows greater stability for cationic and anionic clusters, respectively and also the plot for anionic cluster is similar to the previous study.[21]

3.3 Electron detachment from anionic clusters and ionization of neutral clusters

Using the same level of theory, we have calculated the vertical electron detachment energy (VDE), adiabatic detachment energy (ADE), vertical ionization potential (VIP) and

adiabatic ionization potential (AIP) values of Au_n^-, $Au_nMg_2^-$, Au_n and Au_nMg_2 clusters. It is noteworthy to mention that VDE and ADE values are properties of anions, whereas VIP and AIP are properties of neutral species.

VDE is defined as the energy difference between the neutral clusters at optimized anion geometry clusters and optimized anion clusters, i.e.;

$$VDE = E_{(\text{neutral at optimized anion geometry})} - E_{(\text{optimized anion})} \quad (8)$$

Similarly, ADE is calculated using the following formula:

$$ADE = E_{(\text{optimized neutral})} - E_{(\text{optimized anion})} \quad (9)$$

The other parameter i.e., ionization potential (IP) measures the energy difference between the ground state of the neutral and the ionized clusters. If the ionized cluster has the same geometry as the ground state of the neutral, the ionization energy corresponds to the vertical ionization potential (VIP). On the other hand, the energy difference between the ground state of the cation and ground state of the neutral is referred to as the adiabatic ionization potential (AIP). VIP is generally calculated by using the following formula

$$VIP = E_{(\text{cation at optimized neutral geometry})} - E_{(\text{optimized neutral})} \quad (10)$$

Similarly, AIP is calculated as:

$$AIP = E_{(\text{optimized cation})} - E_{(\text{optimized neutral})} \quad (11)$$

The VDE and ADE values obtained for Au_n^- and $Au_nMg_2^-$ are given in Table 1. The values obtained from our calculations for Au_n^- are in excellent agreement with the previous experimental results.[36] Unfortunately, due to lack of experimental values, it is not possible to make direct comparison on the doped clusters. By plotting the calculated VDE values of bare and doped clusters with respect to cluster size (Fig. S2 of supplementary information), we obtained that the VDE values for the doped $Au_nMg_2^-$ clusters shows even-odd alternation. Also the VDE values decreases significantly for Au clusters when doped with two Mg atoms and the values obtained for even sized clusters are lower than that of their odd counterparts.

The VIP and AIP values obtained for Au_n and Au_nMg_2 are provided in Table 2. The values obtained from our calculations for Au_n are in excellent agreement with the previous experimental results.[37] Due to lack of experimental values, it is not possible to make direct comparison on the doped clusters. The plot of VIP values with respect to cluster size (Fig. S3 of supplementary information) shows even-odd alternation and indicates that the values obtained for odd sized clusters are lower than that of their even counterparts.

3.4 Chemical Hardness

Chemical hardness has been established as an electronic quantity to characterize the relative stability of molecules and aggregates. It is based on the principle of maximum hardness (PMH) proposed by Pearson.[38] It is favored by small-sized atoms, so we can also discuss the stability of our studied clusters on the basis of their hardness. Based on a finite-difference approximation and Koopman's theorem[39] chemical hardness (η) is expressed as:

$$\eta = IPv - EAv$$

where, IP_v is the vertical ionization potential and EA_v is vertical electron affinity. The calculated values of hardness obtained during our calculations are listed in Table 3. The values of hardness obtained for Au_n clusters are in good agreement with the previously reported results.[40] The hardness values for both pure and doped clusters show even odd alternation with respect to cluster size (Fig. S4 of supplementary information). For both the type of clusters, the hardness is higher for even numbered clusters compared to their odd counterparts indicating the greater stability of the former one. The trend of change in hardness is also found to be similar to that of fragmentation energy and second order difference of energy.

3.5 QTAIM analysis

To study the topology of electron density, we have used Bader's quantum theory of atoms in molecules (QTAIM).[28-30] This theory is mainly based on the three dimensional

electron density functions, ρ(r). The topological analysis is the investigation of critical points of this function, ρ(r). The parameters that are commonly used to ascertain the nature and extent of bonding between two atoms are the electron density, ρ and the Laplacian of electron density, $\nabla^2\rho$ at the bond critical point (BCP). Normally, a large value of ρ(r) (>0.2 au) and large and negative value of $\nabla^2\rho$ indicates a covalent or openshell interaction, whereas a small value of ρ(r) (<0.10 au) and a positive value of $\nabla^2\rho$ indicates an ionic or closed-shell interaction. However, this view can not be extended to transition metal complexes since the electron distribution of these elements are diffuse in nature. Hence, in transition metal complexes, the rule is changed and it is generally observed that ρ has a small value and $\nabla^2\rho$ has a small and positive value for a covalent interaction.[41]

The presence of BCP in all the clusters indicates the interaction between the Au and Mg atoms. In QTAIM analysis, we are taken into account only the most stable isomers that are found during geometry optimization. The focus of this QTAIM study was to notice the type of bond involves and the variation of bonding on doping Mg in Au clusters. The different values of the two parameters that we observed during QTAIM are given in Table 4 for some selected most stable bare and doped clusters. The values for the remaining clusters are given in Table S1 of supplementary information.

The small and positive values obtained for ρ and $\nabla^2\rho$ for all the analysed structures in Table 4 indicates the covalent interaction between Au-Au and Au-Mg atoms. However, compared to that of Au-Au bond, bond critical point shifts towards Mg atom in Au-Mg bond as shown in Fig**.** S5 of supplementary information. When we observed the basin paths for the some clusters, Fig. 7, it clearly confirms the interaction between the Au-Au and Au-Mg atoms. Also the presence of ring critical points (RCP) in several clusters confirms the cyclic structures that we obtained during optimisation. For example, we obtained a triangular

structure for cationic Au_3 cluster. The QTAIM analysis confirms this structure by resulting the RCP as shown in A3 of Fig. 7. The conclusion that can be drawn from QTAIM anlaysis is that the studied clusters possess covalent bonds among the bonding atoms. Various smaller values of ρ and $\nabla^2\rho$ obtained for doped clusters compared to that of a pure clusters (Table 4) indicate that the extent of covalent bonding may be strong in the former one.

3.6 Population analysis

The variation of atomic and orbital contributions on doping Mg atoms in Au clusters was oberved by performing population analysis on neutral Au_3 and $AuMg_2$ clusters. The HOMO-LUMO isosurfaces for Au_3 and $AuMg_2$ are shown in Fig. 8. The isosurfaces clearly indicate the formation of π-bonds in both the cases by sidewise overlapping and it support the formation of covalent bond in accordance with our QTAIM study. For Au_3, the atomic contribution is found to be 13% Au + 74% Au + 13% Au and orbital contribution is $0.86(sp^{0.01}d^{0.05})_{Au}$ + $0.51(sp^{0.01}d^{0.02})_{Au}$ + $0.51(sp^{0.01}d^{0.02})_{Au.}$ The percentage of s,p and d-orbitals in Au atom in Au_3 dimer are 94.80, 1.01 and 4.20%, respectively. But on doping two Mg atoms, the atomic contribution changed to 30% Mg + 40% Au + 30% Mg. The orbital contribution is 0.78 $(sp^{0.04})_{Mg}$ + 0.62 $(sp^{1.02}\ d^{0.02})_{Au}$+ 0.78 $(sp^{0.04})_{Mg}$. The percentage of s, p and d-orbitals in Au atom of $AuMg_2$ are found to be 94.31, 1.03 and 4.66%, respectively and that of Mg atoms are 80.48 and 19.52% for s and p-orbtials, respectively. It reveals that there occurs transfer of electron density from p-orbital of Mg atom to the d-orbital of Au-atom which results in increase of the d-orbital electron density. This seems to be the reason for the enhance stability in $AuMg_2$ cluster. When we analysed the Mulliken charges in neutral $AuMg_2$ cluster, it was found that Mg atoms has positive charges (0.477 e) whereas that of gold has negative charges (-0.954). Similarly, for the cationic $AuMg_2$ cluster, Mg atoms possess positive charges (1.041) and Au atoms has negative charge (-1.083) whereras that of anionic $AuMg_2$ clusters have charge 0.048 and -1.096 for Mg and Au atoms, respectively.

This suggests the transfer of charges from Mg atom to Au atom which may arise due to larger electronegativity of Au (2.54) as compared to Mg (1.31).

4. Conclusions

We have presented a systematic study of the structures, stabilities and electronic properties of small bare gold clusters Au_n and bimetallic complexes of doubly Mg doped Au_nMg_2 (charged as well as neutral) using PW91PW91 level of theory. All the results are summarized as follows:

1. Most of the Mg doped Au_n clusters adopt plannar structures. The structures of doped clusters are different to that of pure clusters indicating the effect of doubly doped Mg in the Au clusters.

2. The relative stabilities as a function of cluster size are studied in detail in terms of binding energy per atom, fragmentation energies and second-order difference of energies. These curves show even-odd oscillory behaviours and the calculated results reveal that Au_6, Au_5^+, Au_6^-, Au_4Mg_2, $Au_2Mg_2^+$, $Au_3Mg_2^-$ structures have enhanced chemical stabilities. The stability trends clearly indicates that the studied doped clusters are more stable to that of bare clusters.

3. Ionization potentials and electron detachment energies (both vertical and adiabatic) of Au_n and Au_nMg_2 clusters are discussed and compared with experimental results. Our theoretical results are found to be in good agreement with experimental values. Consequently, our obtained atomic structures of Au_nMg_2 clusters should be reliable. The chemcial hardness values show an oscillatory behaviour and suggests that even numbered clusters are compartivley more stable to that of the odd ones.

4. The QTAIM analysis reveals that the values of electron density, ρ , and its Laplacian, $\nabla^2\rho$ at the Au–Au and Au–Mg BCPs are very small and positive. These two parameters confirm the presence of covalent interactions in the studied clusters. The population analysis suggest the transfer of electrons from Mg to Au atoms. So as a whole we can conclude that the doping of doubly doped Mg can increase the stability of the pure Au clusters.

We hope that the detailed investigation into structures, stability and electronic properties of small bimetallic clusters in the present research work will provide an insight into understanding the larger doped clusters of gold as well as other metals.

Acknowledgements

The work is funded by the Department of Science and Technology, New Delhi in the form of a research project (SR/NM/NS-1023/2011-G). One of the authors, D.B. is thankful to CSIR, New Delhi for providing Senior Research fellowship. The financial support in the form of Dr. D. S. Kothari Post-doctoral fellowship to B.K.M. from University Grants Commission, New Delhi is also acknowledged.

References

1. M. Haruta, T. Kobayashi, H. Samo, N. Yamada, *Chem. Lett*., 1987, **2**, 405.
2. A. Deka and R. C. Deka, *J. Mol. Struc. Theochem*. 2008, **870**, 83.
3. H. Hakkinen, B. Yoon, U. Landman, X. Li, H.J. Zhai and L.-S. Wang, *J. Phys. Chem. A,* 2003, **107**, 6168.
4. N. Shao, W. Huang,W.-N. Mei,L. S. Wang,Q. Wu and X. C. Zeng, *J. Phys. Chem. C,* 2014, **118**, 6887.
5. S. Gilb, P. Weis, F. Furche, R. Ahlrichs and M. M. Kappes, *J. Chem. Phys.*, 2002, **116**, 4094.
6. J. Li, X. Li, H.-J. Zhai, L.-S. Wang, *Science*, 2003, 299, 864. (2003).
7. X. Xing, B. Yoon, U. Landman and J. H. Parks, *Phys. Rev. B*, 2006, **74**, 165423.
8. R. C. Deka, D. Bhattacharjee, A. K. Chakrabartty and B. K. Mishra, *RSC. Adv*., 2014, **4**, 5399.
9. H. Hakkinen and U. Landman, *J. Am. Chem. Soc.*, 2001, **123**, 9704.
10. N. Toshima, H. Yan and Y. Shiraishi, *Metal Nanoclusters in Catalysis and Materials Science*, Elsevier, UK, 2008.
11. F. Maroun, F. Ozanam, O. M. Magnussen and R. J. Behm, *Science*, 2001, **293**, 1811.
12. M. Chen, D. Kumar, C.W. Yi and D. W. Goodman, *Science*, 2005, **310**, 291.
13. H.-Q. Wang, X.-Y. Kuang and H.-F. Li, *Phys. Chem. Chem*. Phys., 2010, **12**, 5156.
14. D. Manzoor, S. Krishnamurty and S. Pal, *J. Phys. Chem. C*, 2014, **118,** 7501.
15. P. Shao, X.-Y. Kuang, Y.-R. Zhao, Y.-F. Li and S.-J. Wang, *J. Mol. Model.*, 2012, **18**, 3553.
16. C.-J. Wang, X.-Y. Kuang, H.-Q. Wang, H.-F. Li, J.-B. Gu and J. Liu, *Comput. Theor. Chem.* 2012, **1002**, 31.

17. D. Bhattacharjee, B. K. Mishra, A. K. Chakrabartty and R. C. Deka, *Comput. Theor. Chem.* 2014, **1034**, 61.

18. http://en.wikipedia.org/wiki/Magnesium.

19. K. Koyasu, Y. Naono, M. Akutsu, M. Mitsui and A. Nakajima, *Chem. Phys. Lett.*, 2006, **422,** 62.

20. C. Majumder, A. K. Kandalam and P. Jena, *Phys. Rev. B*, 2006, **74**, 205437.

21. Y.-F. Li, X.-Y. Kuang, S.-J. Wang and Y.-R. Zhao, *J. Phys. Chem. A*, 2010, **114**, 11619.

22. Accelrys Material Studio 7.0.

23. A. K. Rappé, C. J. Casewit, K. S. Colwell, W. A. Goddard III, W. M. Skiff, *J. Am. Chem. Soc.* 1992, **114**, 10024.

24. S. Antonello, G. Arrigoni, T. Dainese, M. D. Nardi, G. Parisio, L.Perotti, A. Rene´,A.Venzo, and F. Maran, *ACS Nano,* 2014, **8**, 2788.

25. S. E. Huber, C. Warakulwit, J. Limtrakul, T. Tsukudad and M. Probst, *Nanoscale*, 2012, **4**, 585.

26. M.J. Frisch, G.W. Trucks, H.B. Schlegel, G.E. Scuseria, M.A. Robb, J.R. Cheeseman, G. Scalmani, V. Barone, B. Mennucci, G.A. Petersson, H. Nakatsuji, M. Caricato, X. Li, H.P. Hratchian, A.F. Izmaylov, J. Bloino, G. Zheng, J.L. Sonnenberg, M. Hada, M. Ehara, K. Toyota, R. Fukuda, J. Hasegawa, M. Ishida, T. Nakajima, Y. Honda, O. Kitao, H. Nakai, T. Vreven, J.A. Montgomery Jr., J.E. Peralta, F. Ogliaro, M. Bearpark, J.J. Heyd, E. Brothers, K.N. Kudin, V.N. Staroverov, R. Kobayashi, J. Normand, K. Raghavachari, A. Rendell, J.C. Burant, S.S. Iyengar, J. Tomasi, M. Cossi, Rega, N.J. Millam, M. Klene, J.E. Knox, J.B. Cross, V. Bakken, C. Adamo, J. Jaramillo, R.E. Gomperts, O. Stratmann, A.J. Yazyev, R. Austin, C. Cammi, J.W. Pomelli, R. Ochterski, R.L. Martin, K. Morokuma, V.G. Zakrzewski, G.A. Voth, P. Salvador, J.J.

Dannenberg, S. Dapprich, A.D. Daniels, O. Farkas, J.B. Foresman, J.V. Ortiz, J. Cioslowski, D.J. Fox, *Gaussian 09, Revision A.08,* Gaussian, Inc., Wallingford CT, 2009.

27. P. Perdew, J. A. Chevary, S. H. Vosko, K. A. Jackson, M. R. Pederson, D. J. Singh, C. Fiolhais, *Phys. ReV. B*, 1992, **46**, 6671.
28. J. Hay and W. R. Wadt, *J. Chem. Phys*., 1985, 82, 270.
29. P. J. Hay and W. R. Wadt, *J. Chem. Phys*. 1985, 82, 299.
30. H. Xie, X. Li, L. Zhao, Z. Qin, X. Wu, Z. Tang and X. Xing, *J. Phys. Chem. A,* 2012, **116**, 10365.
31. J. Zhou, Z.-H. Li, W.-N. Wang and K.-N. Fan, *J. Phys. Chem. A*, 2006, **110**, 7167.
32. R. F. W. Bader, *Atoms in Molecules: A Quantum Theory,* Oxford University Press: Oxford, U.K. 1990.
33. R. F. W. Bader, *J. Phys. Chem. A*, 1998, **102**, 7314.
34. R. F. W. Bader, *Chem. Rev.* 1991, **91**, 893.
35. AIMAll (Version 13.02.26), Todd A. Keith, TK Gristmill Software, Overland Park KS, USA, 2013 (aim.tkgristmill.com).
36. K. J. Taylor, C. L. Pettiette-Hall, O. Cheshnovsky and R. E. Smalley, *J. Chem. Phys*., 1992, **96**, 3319.
37. M. A. Cheeseman and J. R. Eyler, *J. Phys. Chem.*, 1992, **96**, 1082.
38. R. G. Pearson, *Chemical Hardness: Applications from Molecules to Solids*, Wiley-VCH, Weinheim, 1997.
39. R. G. Parr and W. Yang, *Density functional theory of atoms and molecules*, Oxford University Press, New York, 1989.
40. Y.-R. Zhao, X.-Y. Kuang, B.-B. Zheng, S.-J. Wang and Y.-F. Li, *J. Mol. Model.*, 2012, **18**, 275.
41. L. J. Farrugia, C. Evans and M. J. Tegel, *J. Phys. Chem. A*, 2006, **110**, 7952.

Table 1. Vertical and adiabatic detachment energies of anionic Au_{n+2} and Au_nMg_2 clusters (n=1-5)

	VDE (in eV)			ADE (in eV)		
	Au_{n+2}		Au_nMg_2	Au_{n+2}		Au_nMg_2
n	Calculated	Experimental[32]	Calculated	Calculated	Experimental[32]	Calculated
1	3.59	3.77	1.9	3.56	3.63	1.53
2	2.48	2.63	1.26	2.48	2.48	1.26
3	2.99	2.98	2.13	2.99	2.75	2.12
4	2.02	2.0	1.43	2.02	1.75	1.43
5	2.69	3.38	2.59	2.69	3.13	2.59

Table 2. Vertical and adiabatic ionization potentials of neutral Au_{n+2} and Au_nMg_2 clusters (n=1-5)

	Au_{n+2}			Au_nMg_2	
n	VIP (in eV)	AIP (in eV)	Experimental[33]	VIP (in eV)	AIP (in eV)
1	6.99	6.99	7.27	5.84	5.84
2	7.81	10.2	8.60	6.28	6.28
3	7.06	7.06	7.61	6.36	6.36
4	8.38	8.38	8.80	7.88	7.19
5	6.48	6.48	7.80	6.43	6.43

Table 3. Hardness values of the Au_{n+2} and Au_nMg_2 clusters (n=1-5)

n	Hardness values, (η)		
	Au_{n+2}		Au_nMg_2
	Calculated	Reported[36]	Calculated
1	3.40	5.15	3.94
2	5.32	5.64	5.03
3	4.07	4.51	4.23
4	6.35	6.38	6.45
5	3.79	4.01	3.84

Table 4. Electron density, ρ and the Laplacian of electron density, $\nabla^2\rho$ at the bond critical points (BCP) for some selected clusters.

Cluster	Interaction	ρ	$\nabla^2\rho$
Neutral			
Au_3	Au1 - Au2	0.06	0.15
	Au1 - Au3	0.06	0.15
Au_4	Au2 - Au4	0.06	0.15
	Au1 - Au2	0.05	0.12
	Au2 - Au3	0.05	0.12
	Au1 - Au4	0.05	0.12
$AuMg_2$	Mg1 - Au3	0.03	0.07
	Mg2 - Au3	0.03	0.07
Au_2Mg_2	Mg1 - Au3	0.03	0.1
	Mg2 - Au3	0.03	0.1
	Mg1 - Au4	0.03	0.1
	Mg2 - Au4	0.03	0.1
Cationic			
Au_3	Au1 - Au2	0.06	0.13
	Au1 - Au3	0.06	0.13
	Au2 - Au3	0.06	0.13
Au_4	Au2 - Au4	0.05	0.12
	Au1 - Au2	0.05	0.12
	Au2 - Au3	0.05	0.12
	Au1 - Au4	0.05	0.12
	Au3 - Au4	0.05	0.12

$AuMg_2$	Mg1 - Au3	0.03	0.08
	Mg2 - Au3	0.03	0.08
Au_2Mg_2	Mg1 - Au3	0.03	0.11
	Mg2 - Au3	0.03	0.11
	Mg1 - Au4	0.03	0.11
	Mg2 - Au4	0.03	0.11
Anionic			
Au_3	Au1 - Au2	0.06	0.14
	Au1 - Au3	0.06	0.14
Au_4	Au2 - Au4	0.04	0.1
	Au1 - Au2	0.05	0.12
	Au2 - Au3	0.05	0.12
	Au1 - Au4	0.05	0.12
$AuMg_2$	Mg1 - Au3	0.02	0.06
	Mg2 - Au3	0.02	0.06
Au_2Mg_2	Au1 - Mg3	0.02	0.07
	Au2 - Mg3	0.02	0.07
	Au1 - Mg4	0.02	0.07
	Au2 - Mg4	0.02	0.07

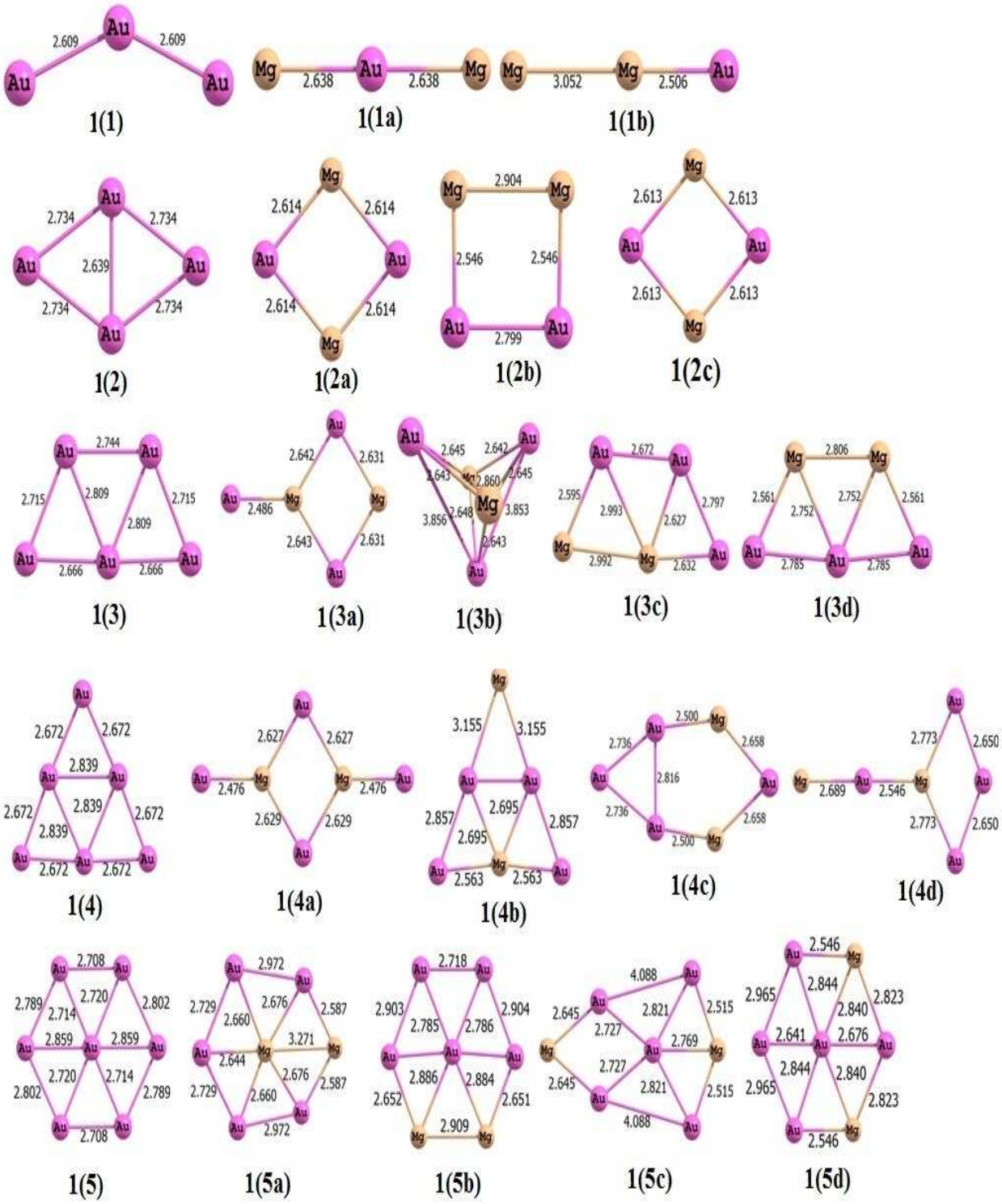

Fig. 1. Optimized structures of neutral Au_{n+2} and Au_nMg_2 (n = 1–5) clusters

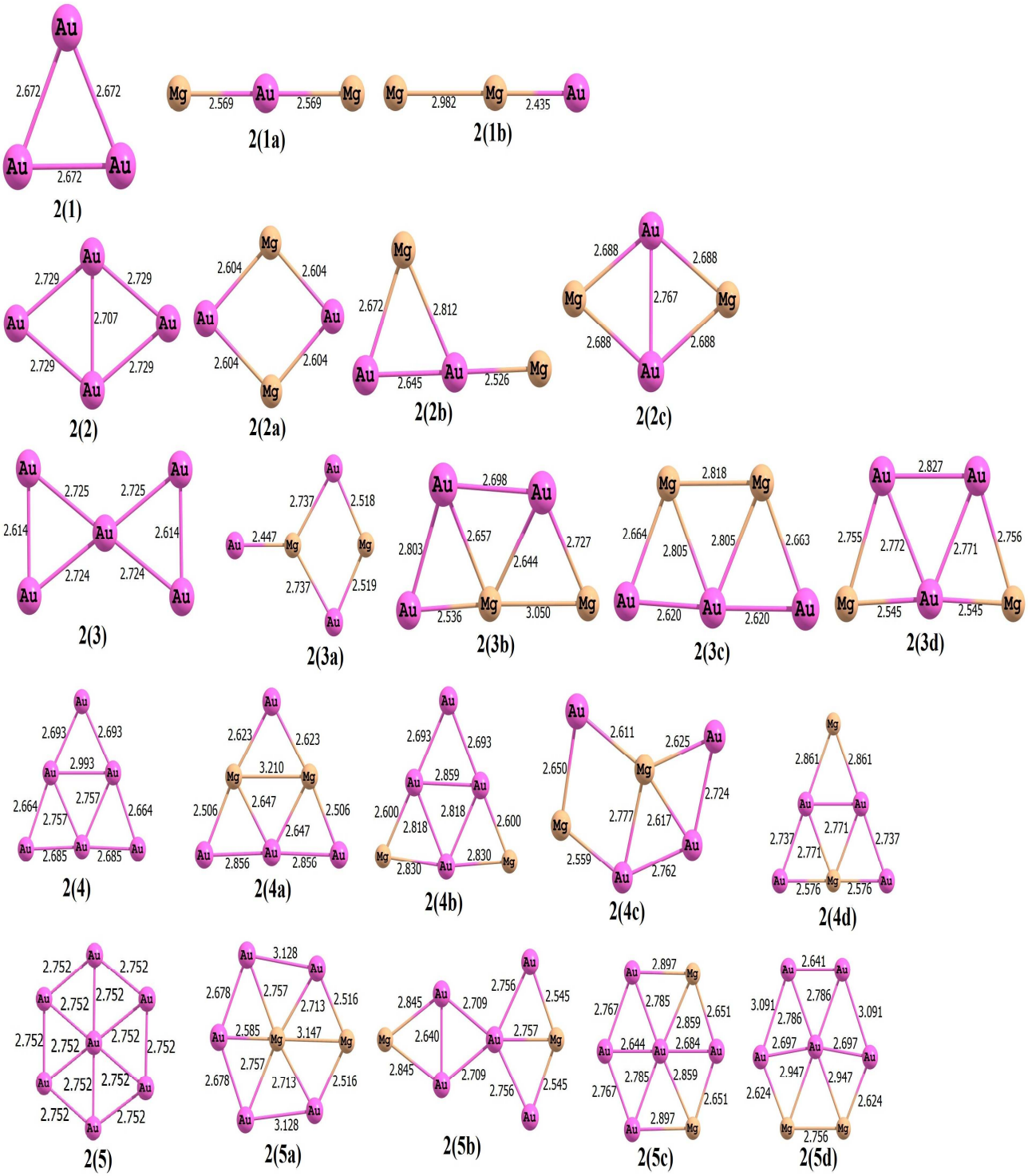

Fig. 2. Optimized structures of cationic Au_{n+2} and Au_nMg_2 (n = 1–5) clusters.

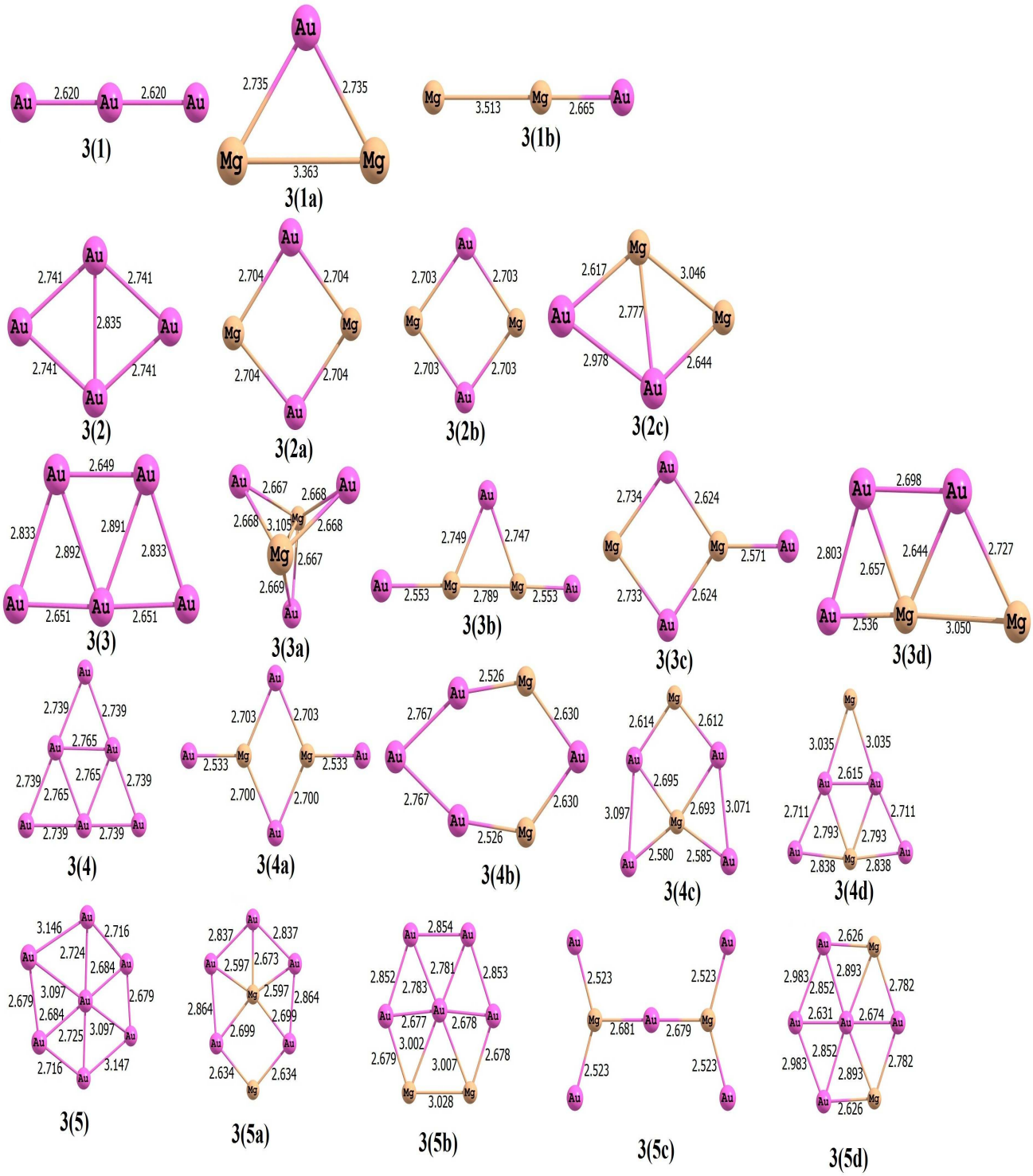

Fig. 3. Optimized structures of anionic Au_{n+2} and Au_nMg_2 (n = 1–5) clusters.

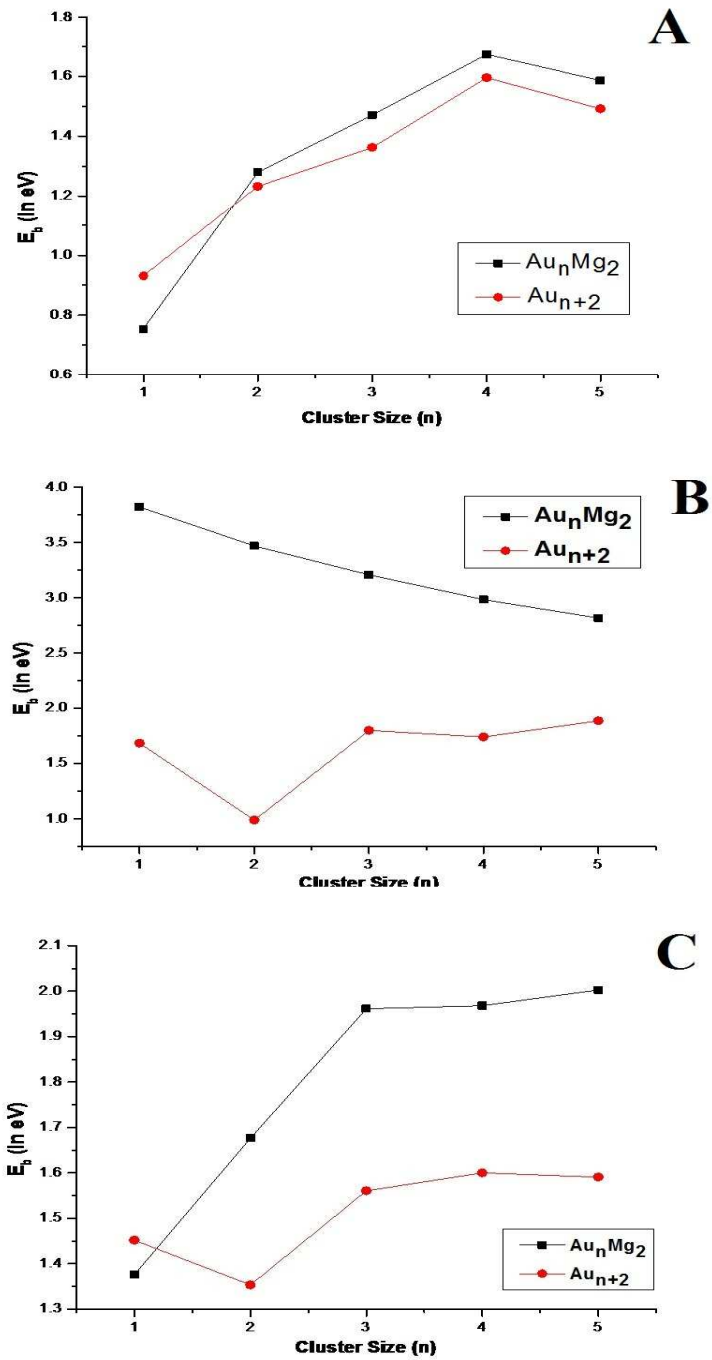

Fig. 4. Variation of binding energies with respect to cluster size for (A) neutral, (B) cationic and (C) anionic clusters in bare and magnesium doped gold clusters.

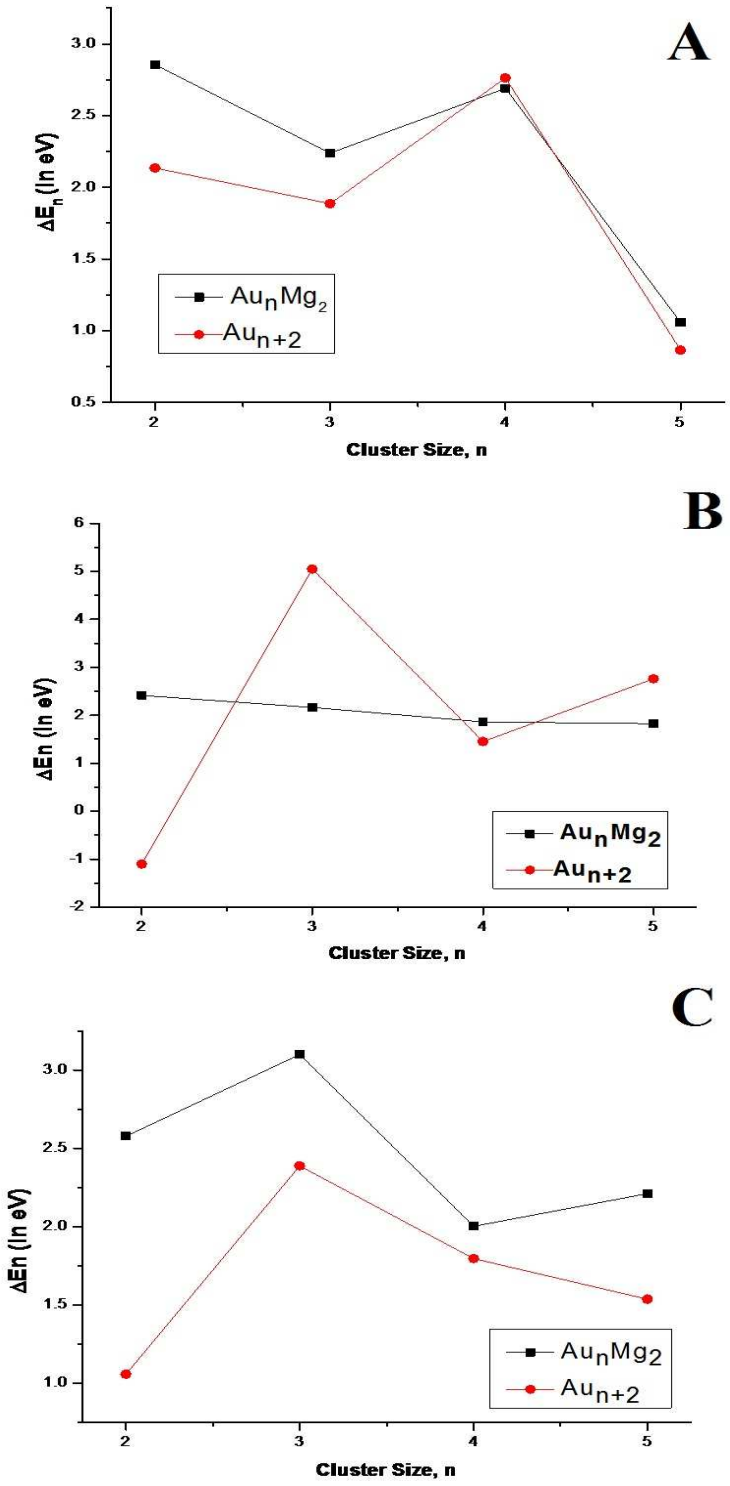

Fig. 5. Variation of fragmentation energies with respect to cluster size for (A) neutral, (B) cationic and (C) anionic clusters in bare and magnesium doped gold clusters.

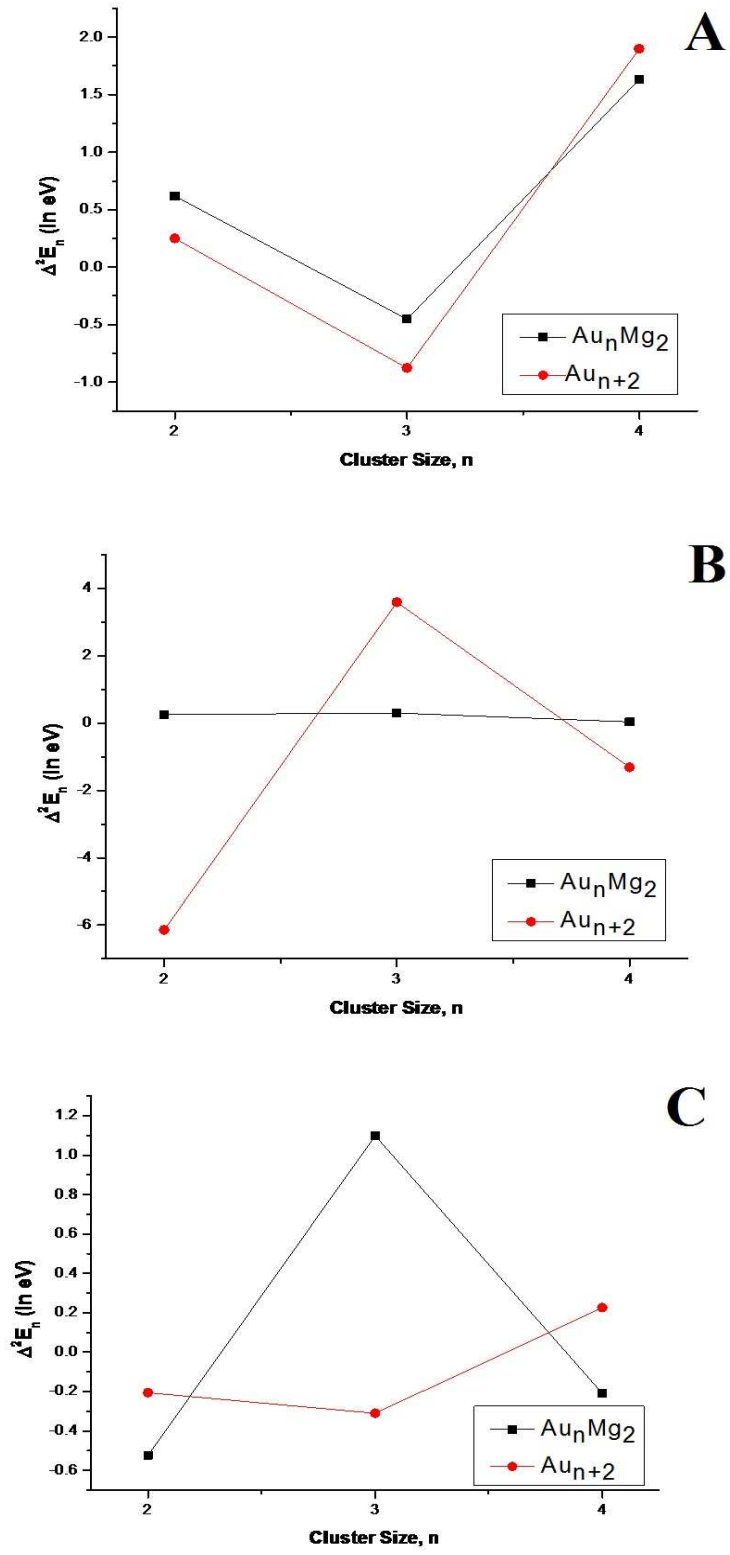

Fig. 6. Variation of second order difference of energies with respect to cluster size for (A) neutral, (B) cationic and (C) anionic clusters in bare and magnesium doped gold clusters.

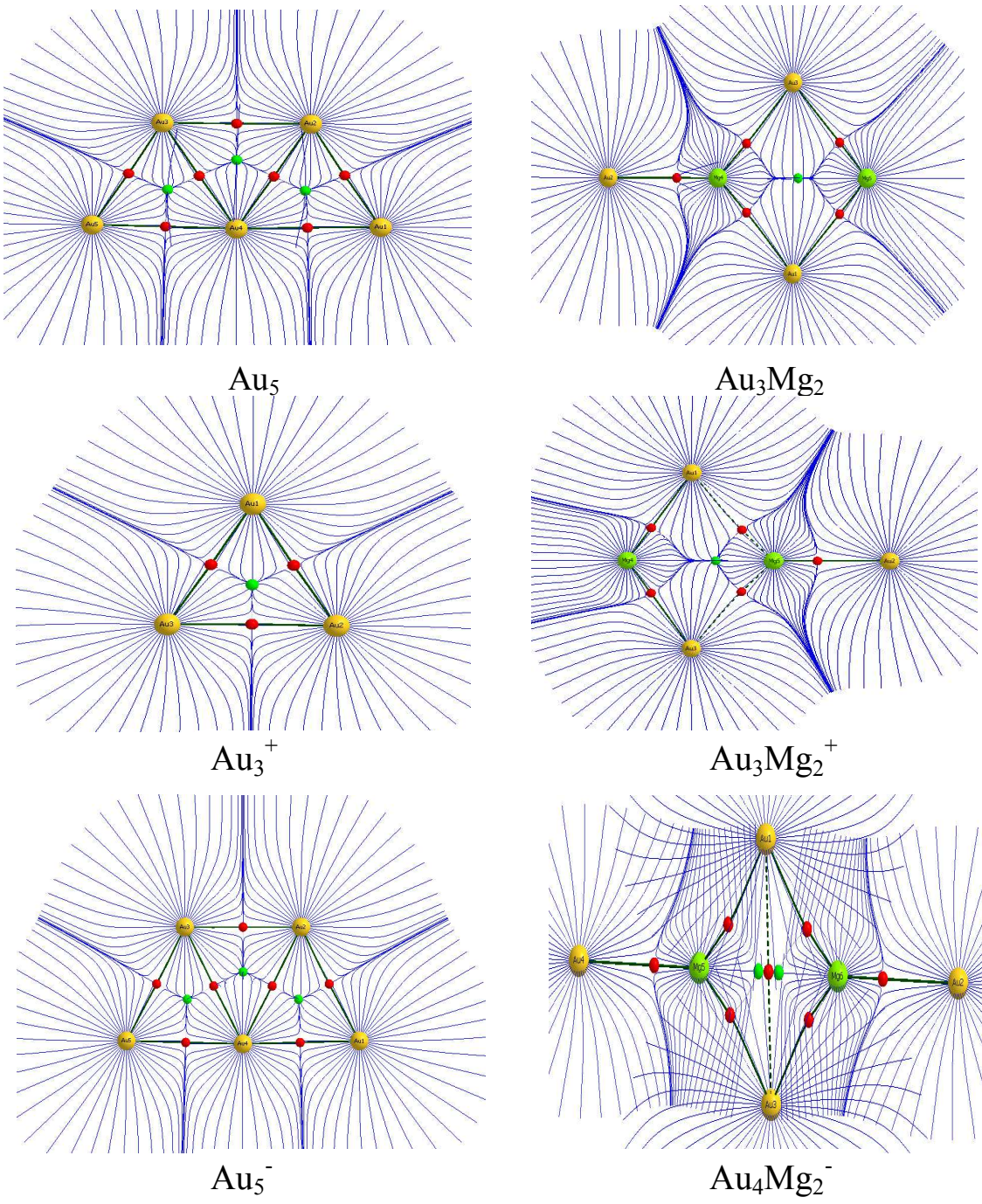

Fig. 7. Trajectory field in some of the Au_n and Au_nMg_2 clusters. Gold and magnesium atoms are represented by yellow and green spheres respectively. Bond paths and basin paths are indicated by dark green and blue lines, while the interatomic surfaces are indicated by dark blue lines. Red and green dots indicate bond critical points and ring critical points, respectively.

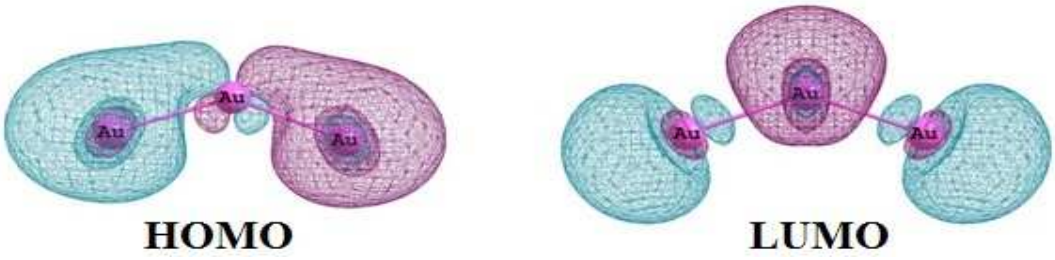

Atomic Contribution: 13% Au + 74% Au + 13% Au

Orbital Contribution: $0.86(sp^{0.01}d^{0.05})_{Au} + 0.51(sp^{0.01}d^{0.02})_{Au} + 0.51(sp^{0.01}d^{0.02})_{Au}$

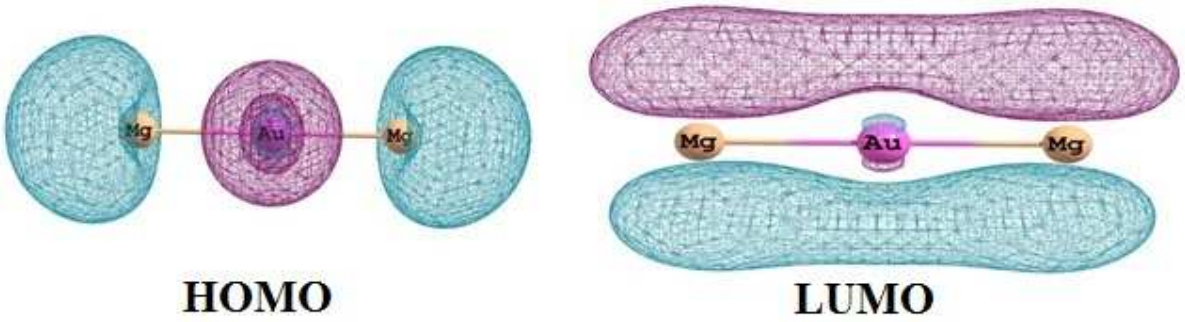

Atomic Contribution: 30% Mg + 40% Au + 30% Mg

Orbital Contribution: $0.78\ (sp^{0.04})_{Mg} + 0.62\ (sp^{1.02}\ d^{0.02})_{Au} + 0.78\ (sp^{0.04})_{Mg}$

Fig. 8. HOMO and LUMO isosurfaces of Au_3 and $AuMg_2$ clusters.